

**JYX**



**This is a self-archived version of an original article. This version may differ from the original in pagination and typographic details.**

**Author(s):** Frimodig, Janne; Haukka, Matti

**Title:** Removal of estrogens from aqueous solutions using 3D-printed polymers

**Year:** 2023

**Version:** Published version

**Copyright:** © 2023 The Author(s). Published by the Royal Society of Chemistry

**Rights:** CC BY 3.0

**Rights url:** <https://creativecommons.org/licenses/by/3.0/>



**Please cite the original version:**

Frimodig, J., & Haukka, M. (2023). Removal of estrogens from aqueous solutions using 3D-printed polymers. *Environmental Science : Advances*, 2(12), 1739-1745.  
<https://doi.org/10.1039/D3VA00159H>



Cite this: DOI: 10.1039/d3va00159h

# Removal of estrogens from aqueous solutions using 3D-printed polymers†

Janne Frimodig  and Matti Haukka \*

Different pharmaceuticals and endocrine-disrupting chemicals (EDCs) can negatively impact our environment, even at nanogram per liter levels. At the same time, the amount of micro- and nanoplastics from various sources, such as personal care products, wastewater sludge, vehicle tire wear, etc., are increasing in the environment. Polymers may also serve as a source for EDCs and other contaminants *via* the decomposition of polymers or metabolic processes. However, they may serve as sorbents for pollutants as well. In this work, estrogen group hormones were shown to bind into 3D-printed filters made from commonly used polymers, such as polyamide-12 (PA), thermoplastic polyurethane (TPU), polypropylene (PP), and polystyrene (PS). The adsorption tests showed that polymers containing a higher degree of functional groups (PA and TPU) were more efficient adsorbents than structurally simpler polymers (PP and PS). Kinetic models for polyamide flow-through filters were measured for estrone, 17 $\beta$ -estradiol, and 17 $\alpha$ -ethinylestradiol. The filters printed with the powder-bed fusion 3D printing technique successfully removed estrogen group hormones from water. The 3D printing technique provided a versatile tool for preparing filters with optimized porosities and flow-through properties.

Received 9th June 2023  
Accepted 25th October 2023

DOI: 10.1039/d3va00159h

rsc.li/esadvances

## Environmental significance

Our environment struggles with ever-increasing amounts of pharmaceuticals, personal care products, cosmetic products, and microplastics. The harmfulness of polymer waste is not limited to only ingestion and bioaccumulation, as chemically functional materials can pose additional hazards. In this study, we have studied several common polymers and their ability to bind estrogen-group hormones, which as endocrine-disrupting chemicals, can pose serious health hazards to animals and humans. We found that functionally active polymers such as polyamide (PA, nylon) and thermoplastic polyurethane (TPU) adsorb these compounds at significant levels. We also manufactured functionally active 3D-printed adsorbents using these materials, which can be used to purify contaminated waters, highlighting upcycling and reusability as a viable solutions.

## 1 Introduction

Endocrine-disrupting chemicals (EDCs) continually challenge the current environment and habitats with long-lasting effects.<sup>1</sup> Humans and animals excrete hormones, such as estrone (E1), 17 $\beta$ -estradiol (E2), and estriol (E3), which can create considerable environmental burden if not addressed accordingly.<sup>2,3</sup> This environmental impact is exacerbated by the widespread use of similar synthetic compounds such as 17 $\alpha$ -ethinylestradiol (EE2), which has been reported to cause harmful effects even in nanogram per liter concentrations.<sup>4,5</sup> Furthermore, the overall steroid emissions are estimated to rise 10% annually, which highlights the need for improved purification processes.<sup>6</sup>

Major contributors to EDC-related waste are municipal waste and agricultural sources.<sup>7,8</sup> The 2015 data revealed that from

yearly total steroid excretion of 20 440 t, more than 70% was produced by animals, especially cattle.<sup>6</sup> Agricultural hotspots have increased concentrations of EDCs in soil, which are products of livestock's naturally produced hormones but are also caused by the continuous reuse of manure in agricultural fertilization.<sup>9</sup> Improper or inefficient waste treatment increases contaminants' levels even higher, highlighting the importance of efficient wastewater treatment facilities.<sup>6</sup> Researchers have estimated that the reuse of purified wastewater in irrigation, agriculture, and drinking water will rise in the future.<sup>10</sup>

Currently, wastewater treatment facilities utilize combinations of processes, such as membrane bioreactors,<sup>11</sup> nano-filtration,<sup>12</sup> and different types of oxidations,<sup>13</sup> along with more conventional sedimentation and adsorption techniques. Advances with different hybrid adsorbent materials have also been made.<sup>14,15</sup> Unfortunately, the removal of pharmaceuticals, hormones, and other harmful EDCs is not perfect, and small quantities of compounds pass through unscathed<sup>16</sup> or form different, but still potentially harmful, metabolic and other by-products.<sup>17</sup> Furthermore, using additional purification

Department of Chemistry, University of Jyväskylä, P.O. Box 35, FI-40014 Jyväskylä, Finland. E-mail: matti.o.haukka@jyu.fi

† Electronic supplementary information (ESI) available. See DOI: <https://doi.org/10.1039/d3va00159h>



techniques adds complexity and operational costs to wastewater facilities.

Different filtration processes can provide a cost-effective way to handle large volumes and low contaminant concentrations. However, one of the drawbacks of conventional filtration by adsorbents, such as activated carbon, is inherently low selectivity, resulting in the co-extraction of other unwanted compounds and, thus, faster saturation. Unfortunately, the saturated material is usually disposed of by burning, which prevents any reuse of extraction material and ultimately increases operational costs. Therefore, other materials should be considered for purification purposes.

Commonly used polymers can contain residues of harmful additives, which can leach out into the environment<sup>18,19</sup> but given suitable conditions, they can also adsorb such substances, including metal ions and molecular compounds.<sup>20–22</sup> If such contaminated polymers end up in the organisms, for example, through the consumption of microplastics, it can significantly increase the environmental damage caused by plastics.<sup>23</sup> Conversely, it is possible to utilize the ability of polymers to bind ions and compounds to themselves and use them as adsorbents. The aim of this work is, on the one hand, to investigate the ability of polymers to adsorb estrogen hormones and additionally, to seek to exploit the adsorption properties of polymers to remove hormones from the aquatic environment. 3D printing provides an excellent tool for utilizing different polymers in the manufacturing of adsorbent filters.

Selective laser sintering (SLS) is a widely used powder-bed fusion 3D printing technique in producing prototypes and other objects from various polymeric materials. In the SLS technique, a laser is used to selectively sinter thermoplastic particles together layer by layer, ultimately forming an object with the desired size, shape, porosity, and mechanical properties. Usually, the main focus is on the physical strength and durability of the printed objects. However, selective laser sintering can also be used to manufacture chemically active and porous objects by choosing suitable printing material and controlling laser sintering parameters.<sup>24–26</sup> The input energy densities commonly used to manufacture solid objects are typically higher than what is used to produce porous objects. By using lower energy densities, the polymer particles are not completely melted. Instead, they retain their particle-like appearance, generating voids between the particles.<sup>27,28</sup> This type of additive printing uses typically powdered substances, such as polyamide-12 or thermoplastic polyurethane, which can be modified with additional pretreatment or by simply physically mixing supporting polymer with a functional component prior printing process.<sup>24,29</sup>

3D-printed scavenging filters have been previously effectively deployed in removing inorganic and organic materials.<sup>20,21,29–31</sup> However, the use of 3D-printed filters with polymers containing different types of functional groups in the selective removal of the most important estrogens has not been screened so far. This study aims to fill that lack of knowledge by exploring using commonly used 3D printing polymers as the adsorbent materials for estrogen group hormones.

## 2 Materials and methods

### 2.1 Materials and chemicals

The materials obtained for chromatographic measurements were gas chromatography (GC) or ultra-high performance liquid chromatography (UHPLC) grade. Ammonium fluoride (>99.99%) was bought from Merck. Estrone (E1), 17 $\beta$ -estradiol (E2), estriol (E3), and 17 $\alpha$ -ethinylestradiol (EE2) were purchased from TCI Europe with purity greater than 98%. Stock solutions containing 1 g L<sup>-1</sup> and 10 mg L<sup>-1</sup> of steroid were prepared using methanol. Calibration solutions containing all studied steroids were diluted from stock solutions using methanol. A synthetic sample solution containing approximately 0.5 mg L<sup>-1</sup> of each hormone was diluted in ultrapure water. All solutions were stored in +4 °C. The printing polymers polystyrene (Coathylene Sint PS, PS) was obtained from Axalta Coating Systems Ltd, thermoplastic polyurethane (Ultrasint TPU 88A, TPU), and polypropylene (Ultrasint PP nat 01, PP) was purchased from BASF SE and Polyamide-12 (PA2200, PA) was obtained from EOS GmbH. All printing materials were used in the printing process as is, without any pretreatment. The printed filters were washed with methanol and water prior to use. The detailed printing parameters can be found in ESI Table 1.† Activated carbon with a granular size of approximately 0.4–1.2 mm was bought from a retail store and ground into a more homogenous size using a Fritsch ball mill. Ultrapure water (18.2 M $\Omega$  cm) was purified using Elga Purelab Ultra, and it was used in dilutions and all washing steps. The experiments were conducted in pH range 5–7.

### 2.2 Filter manufacturing process

The cylindrical filters with a height of 5 mm and diameter of 16 mm were designed using FreeCAD and prepared for instrument using Slic3r slicing software before manufacturing them in batches using Sharebot SnowWhite SLS 3D-printer. Slight differences in the weight of the filters (0.5–0.7 g) were observed, mainly due to the molecular weights of different printing materials. Different laser powder ( $P$ ; W), hatching space ( $hs$ ; mm), and laser speed ( $v$ ; mm s<sup>-1</sup>) settings used in the printing process can be summarized using energy density (ED; J mm<sup>-2</sup>), which enables fast comparisons of energies required to produce porous filters using the following eqn (1).

$$ED = \frac{P}{hs \times v} \quad (1)$$

The energy densities used in the printing process were lower than 100 mJ mm<sup>-2</sup> for all materials. The more detailed printing parameters are shown in ESI Table 2.†

### 2.3 Sorption and breakthrough studies

All experiments were conducted in flow-through systems, where each filter could be subjected to a fixed flow rate and volume. For each polymer, a printed filter with a volume of 1 ml was tightly fit in the middle of a 10 ml syringe so that both faces of the filter were unobstructed, and liquid could only flow through the filter. A multihormone sample solution with known



concentrations of approximately  $0.5 \text{ mg L}^{-1}$  was pumped through with a flow rate of  $10 \text{ ml min}^{-1}$ . Samples were gathered with intervals of 1, 2, 5, 10, 20, 30, 40, 50, and 60 min, which formed a total volume of 600 ml or 600 bed volumes. This would mean that approximately  $300 \text{ }\mu\text{g}$  of each hormone would have been filtered through the adsorbent material. The samples were analyzed without any additional treatment using liquid chromatography. All experiments were conducted using 4 replicates.

## 2.4 Elution studies

Prewashed filters were loaded using 20 ml of approximately  $0.5 \text{ mg L}^{-1}$  multihormone solution. The adsorbed amount was calculated from the difference between the initial and final concentrations. Filters were then washed with 20 ml of ultra-pure water and 20 ml of methanol with a  $2 \text{ ml min}^{-1}$  feed rate. The total volume of 20 ml was collected and measured from each test run in triplicates.

## 2.5 Kinetics modeling

The adsorption kinetics of data obtained from the continuous flow breakthrough experiment were studied using linearized and non-linearized pseudo-first-order and pseudo-second-order kinetic models. The aim was to gain insight into the capacity of printed polymers. The linearized pseudo-first-order and pseudo-second-order equations are shown in eqn (2) and (3) as follows:

$$\frac{dq_t}{dt} = k_1(q_e - q_t) \quad (2)$$

$$\frac{dq_t}{dt} = k_s(q_e - q_t)^2 \quad (3)$$

where  $q_t$  ( $\text{mg g}^{-1}$ ) is the amount of adsorbate adsorbed at time  $t$  (min),  $q_e$  ( $\text{mg g}^{-1}$ ) is adsorbed material at equilibrium and  $k_1$  ( $\text{min}^{-1}$ ) and  $k_s$  ( $\text{g (mg min}^{-1})^{-1}$ ) are pseudo-first-order and pseudo-second-order rate constants, respectively.<sup>32</sup>

The non-linearized equations for pseudo-first-order (Fig. 4) and pseudo-second-order (Fig. 5), respectively were

$$q_t = q_e(1 - e^{-k_1 t}) \quad (4)$$

$$q_t = \frac{k_2 q_e^2 t}{1 + k_2 q_e t} \quad (5)$$

where  $k_1$  ( $\text{h}^{-1}$ ) and  $k_2$  ( $\text{g mg}^{-1} \text{ h}^{-1}$ ) are sorption rate constants for pseudo-first-order and pseudo-second-order models.<sup>22</sup>

## 2.6 Liquid chromatography-mass spectroscopy

Agilent 1290 Infinity UHPLC system coupled with Agilent 6460 Triple Quadrupole-mass spectrometer was used for quantitative analysis. EclipsePlus C18 RRHD ( $2.1 \text{ mm} \times 50 \text{ mm } 1.8 \text{ }\mu\text{m}$ ) was used in preliminary and breakthrough studies, while Kinetex Biphenyl ( $2.1 \text{ mm} \times 50 \text{ mm } 1.7 \text{ }\mu\text{m}$ ) was used in elution and reusability studies. Both columns were kept at  $30 \text{ }^\circ\text{C}$  during the measurement. The analyte detection was conducted using Multiple Reaction Monitoring (MRM). Two transitions of each hormone were considered for quantification and qualification

purposes. Ion spray voltage was set to 4000 V and source temperature to  $500 \text{ }^\circ\text{C}$ . The five-point calibrations for all hormones were conducted from  $100 \text{ }\mu\text{g L}^{-1}$  to  $1000 \text{ }\mu\text{g L}^{-1}$ , and a good linearity of  $R^2 > 0.999$  was obtained for all analytes. Instrumental parameters are shown in detail in ESI Table 3.† The mobile phase with the C18 column was  $\text{H}_2\text{O} + 1 \text{ mM NH}_4\text{F}$  as A solvent and 35% acetonitrile with 65% methanol as B solvent. The mobile phase gradient was initially held at B: 20% for 0.5 minutes, after which B was raised to 70% in 7 minutes. Lastly, B: 70% was held for 3 minutes resulting in a run time of 10 minutes. A  $0.3 \text{ ml min}^{-1}$  flow rate with a sample injection volume of  $5 \text{ }\mu\text{l}$  was used. For biphenyl column isocratic run with 40 : 60 v/v% of A:  $\text{H}_2\text{O}$  and B: 35% acetonitrile with 65% methanol was used with a flow rate of  $0.1 \text{ ml min}^{-1}$  with a runtime of 10 min.

## 2.7 Scanning electron microscopy

Scanning electron microscope (SEM) analysis was conducted with Zeiss EVO-50XVP. An acceleration voltage of 15 kV and a working distance of 9 to 9.5 mm were used to perform imaging. All samples were coated with a thin layer of gold using a gold sputter machine before analysis.

# 3 Results and discussion

The functional differences of several thermoplastic polymers in removing hormones (Fig. 1) were studied with synthetic sample solutions. The hydrophobicity and functional groups of the polymer play a significant role in removal capabilities, as previously pointed out by several research groups.<sup>31,33-35</sup>

The 3D-printed filters in this study contained voids and channels formed by partially sintered, nonporous particles with an average diameter of *ca.*  $50 \text{ }\mu\text{m}$ . The resulting voids can be magnitude larger than what is found in typical liquid chromatography columns. Therefore, the effect of size exclusion was not considered to have a significant role in capturing hormones. Furthermore, hydrophilic materials containing a large number of possible hydrogen bonding sites can form hydrogen bonds with water molecules which can hinder flow and cause retention.<sup>36</sup> This effect decreases as the size of channels increases.

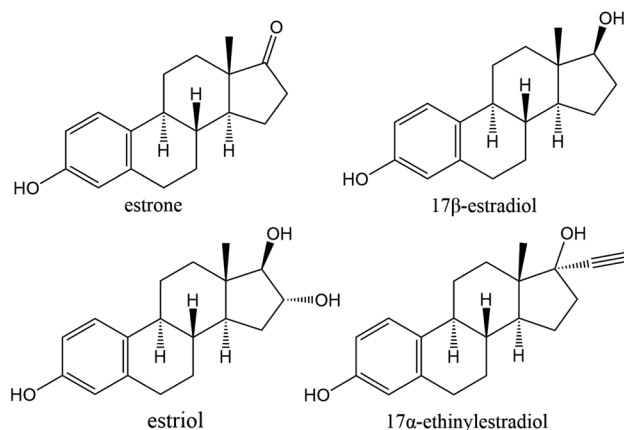


Fig. 1 Structures of estrogens used in the study.





Hydrophobic interactions seemed to play only a minor role in sorption systems studied in this study. This might be caused by a higher concentration of hormones compared to what is typically present in wastewater effluents. However, these experiments aimed to find the saturation point of the polymeric adsorbents within a reasonable timescale and volume of solution.

### 3.1 Surface morphology

The partially sintered particles form voids and flow channels in the filter when low input energy densities are used, which enables efficient adsorption through flow-through systems (Fig. 2). The physical properties can be customized by altering the input energy density and, therefore, the filters' porosity.<sup>20,26</sup> These include but are not limited to overall structural integrity, modification of back-pressure, and flow-speed characteristics of the filters. While the inner structure of the polymer particle in printed filters is inaccessible for diffusion, the active functional groups on the outer surface of the partially sintered polymer particles can bind organic material. An overview of the polymers used in this study can be found in Table 1 and structures of TPU and PA12 can be found in ESI Fig. 1 and 2,<sup>†</sup> respectively.

Compounds can adhere to a surface of printed material using electrostatic interactions of charge-based binding if the pH of the solution enables deprotonation of compounds. Therefore,  $pK_a$  values provide valuable information about how binding could happen, which are around 10–11 for the estrogens.<sup>38</sup> This would mean that in the slightly acidic pH range of 5–7 used in this study, all hormones would be in their neutral form. Thus, binding through charge-based binding or ion exchange mechanisms is unlikely, but some hydrophobically assisted ion exchange can occur.<sup>39</sup> The estrogens studied in this paper have strong hydrogen bond acceptor and donor capabilities through hydroxyl groups, strong acceptor capability through ketones, and are weak  $\pi$  acceptors using aromatic rings.

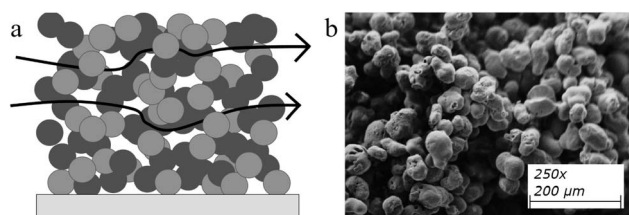


Fig. 2 (a) Simplified cross-section of 3D-printed material showing solvent flow-through. (b) Break surface of polyamide-12 filter under 250 $\times$  magnification imaged using scanning electron microscope image.

Table 1 Base polymers

| Polymer          | Manufacturer               | Melting point, °C |
|------------------|----------------------------|-------------------|
| Polyamide-12     | EOS GmbH                   | 176–183 (ref. 37) |
| Polystyrene      | Axalta Coating Systems Ltd | 105 (ref. 37)     |
| Polypropylene    | BASF SE                    | 125–140 (ref. 37) |
| Polyurethane 88A | BASF SE                    | 160 (ref. 37)     |

The tested adsorbent materials provide a wide variety of different functional groups. Polyamide-12 and polyurethane contain hydrogen bond acceptors and donors in the form of amide groups. Furthermore, polyurethane and polystyrene include arene rings, which can act as hydrogen bond acceptors for estrogens. From selected materials, polypropylene provided a good benchmark for this study as it does not contain functional groups suitable for hydrogen bonding while still having similar hygroscopic properties with the other studied polymers.<sup>35,40</sup> The results were compared with well-known general adsorbent, *i.e.*, porous activated carbon. Therefore, activated carbon was used as an additive material with polyamide-12 (ACPA). The problem with activated carbon is that it is non-selective and non-reusable, which ultimately means faster saturation of the material and undesirable disposal by burning. Here activated carbon was used as a comparison against other printing materials.

Retention by size exclusion, one of the common retention methods of filtration, is an unlikely event for these polymers, as partially sintered particles form typically relatively large, micrometer-scale flow channels. However, charge repulsion,

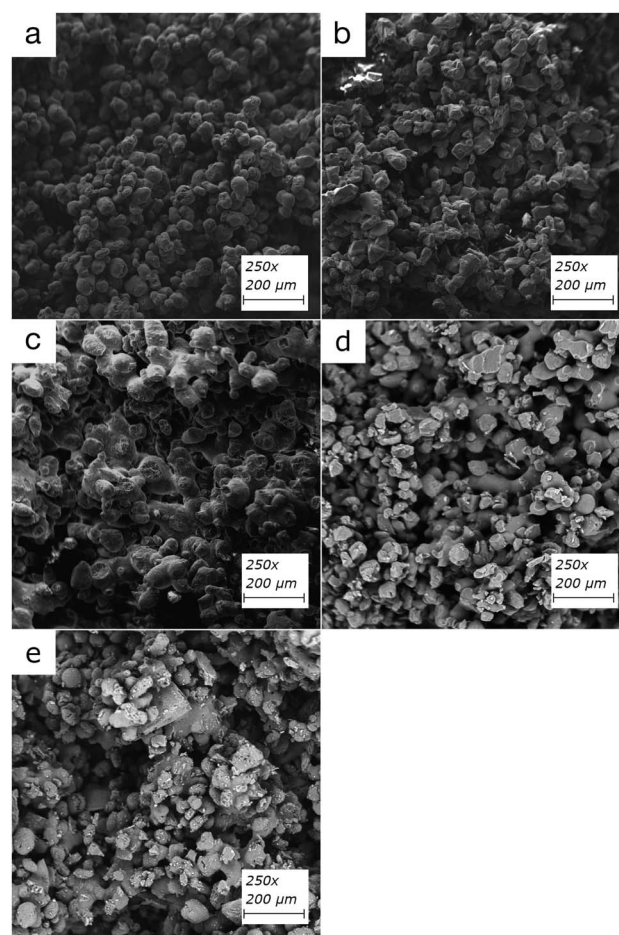


Fig. 3 Scanning electron microscope images of break surfaces of (a) polyamide-12, (b) polystyrene, (c) thermoplastic polyurethane, (d) polypropylene, and (e) 30 wt% activated carbon additive on polyamide-12 filters with under 250 $\times$  magnification.



adsorption, and sorption diffusion with the surface of sintered particles are likely to happen. The break surface of each printed filter was imaged using SEM (Fig. 3) to confirm the porous structure.

### 3.2 Breakthrough studies

The breakthrough curves provide information about the effectiveness and capacity of sorbent material. The breakthrough curve studies were conducted with the cylindrical filters, which had a height of 5 mm and diameter of 16 mm resulting in a total volume of 1 ml (1 bed volume, BV). Breakthrough experiments suggest that further experiments with reusability should be conducted with volumes less than 20 BV. After this, the material becomes more saturated, and hormonal concentrations in effluent increase, as seen from Fig. 4. This does not seem to happen with TPU and ACPA during our experiment. The most promising materials were PA and TPU, which had similar capabilities as baseline material ACPA, and further studies were focused on these materials in mind.

Materials showed only limited selectivity, from which most notable was the inability to retain estriol, which passed all but activated carbon-doped material with minimal adsorption. High efficiency of activated carbon was expected as it is widely used in the purification and removal of hormonal material.<sup>41</sup> Our results showed that activated carbon could easily be incorporated into the 3D-printed filters simply by mixing it with a suitable supporting polymer. The activated carbon is attached to the surfaces of the partially sintered polymer particles. Therefore, it is available for adsorption and not encapsulated by the supporting polymer.

### 3.3 Elution studies

Elution studies showed that even a relatively small amount of 20 ml of methanol could desorb hormones from polymers with

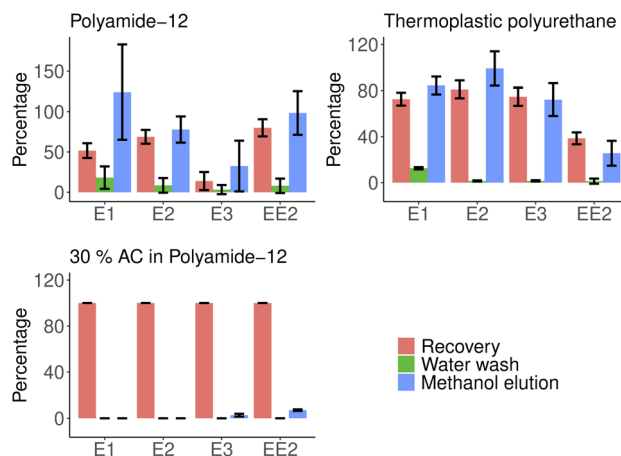


Fig. 5 Elution efficiencies of water and methanol in removing estrogen group hormones from polymers.

varying efficiency. Washing steps with water does not release a significant part of the bound material. Fig. 5 shows the extraction efficiency of different materials and the efficiency of follow-up elution steps compared against extracted masses. Total extraction could be obtained with multiple washing steps without losing adsorption capabilities of the filters. Acetone was found to break filters and increase elution efficiency with a cost of reusability. The activated carbon-doped filters proved to be the most efficient adsorbents while preventing virtually any desorption when washed with water and methanol. More detailed information is available in ESI Table 4.†

### 3.4 Kinetics modeling

The experimental setup used with kinetics modeling deviates from the more commonly used one as a known concentration of the solution was pumped through the 3D-printed filter with

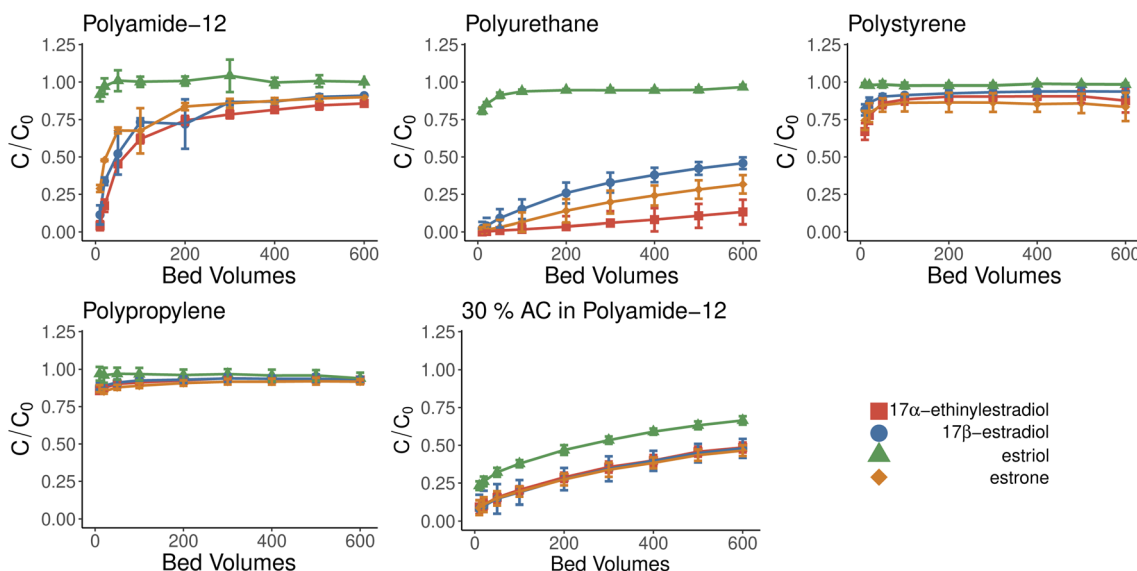


Fig. 4 Breakthrough curves for polyamide-12, polyurethane, polystyrene, polypropylene and 30 wt% of activated carbon in polyamide-12 with fixed  $10 \text{ ml min}^{-1}$  flow rate,  $0.5 \text{ mg L}^{-1}$  initial concentration and bed volume of 1 ml.



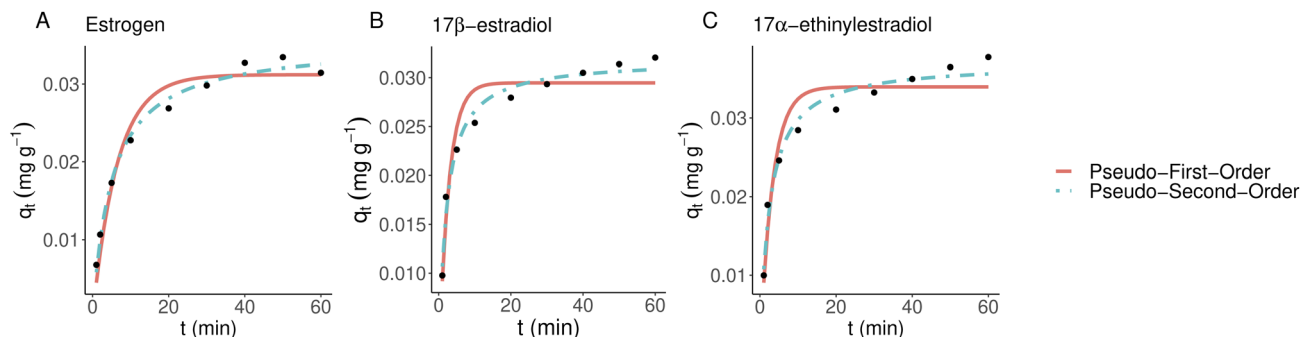


Fig. 6 Non-linearized pseudo-second-order kinetics plots of (A) estrogen, (B) 17 $\beta$ -estradiol and (C) 17 $\alpha$ -ethinylestradiol with polyamide-12 with fixed 10 ml min<sup>-1</sup> flow rate, 0.5 mg L<sup>-1</sup> initial concentration and bed volume of 1 ml.

Table 2 Non-linearized pseudo-second-order model parameters obtained with polyamide-12

| Compound                      | $k_2$     | $q_e$     |
|-------------------------------|-----------|-----------|
| Estrogen                      | 5.6007103 | 0.0352706 |
| 17 $\beta$ -Estradiol         | 15.82     | 0.03186   |
| 17 $\alpha$ -Ethinylestradiol | 11.03     | 0.03706   |

a known speed. This can lead to an adsorbate-constricted environment and a static model could be obtained using an additional constant. Unlike thermoplastic polyurethane and activated carbon-doped polyamide, the kinetics models were tested only with polyamide-12 as it reached saturation. Fig. 4 shows adsorbed material bound over time which supports the observations that estriol does not bind with polyamide-12. Therefore, it was excluded from further models. Non-linearized pseudo-first-order and pseudo-second-order models are shown in Fig. 6 and Table 2 for polyamide-12 with the latter following the experimental results more closely. The more detailed results from non-linearized and linearized data can be found in ESI Tables 5 and 6.†

## 4 Conclusions

In this paper, we have shown that commonly used plastics such as polyamide-12, thermoplastic polyurethane, polystyrene, and polypropylene interact with the estrogen group compounds differently depending on the number and nature of the functional groups of the polymer. Polymers that contain no or only a limited number of functional groups suitable for hydrogen bonding were found to be relatively inert in retaining studied hormones. However, other weak interactions are possible, and some sorption occurs even with these polymers.

Polyamide-12 and thermoplastic polyurethane, which both contain higher amounts of suitable functional groups, efficiently captured most of the studied estrogen hormones. However, estriol was not captured by any of the tested polymeric materials, even though estriol can form hydrogen bonds through its hydroxy groups. This may be due to estriol's preference to form hydrogen bonds with other compounds and

solvent water, using its OH-groups in positions 16 and 17. If these interactions dominate, interactions with the polymer are limited to weaker physisorption. The results are in line with previous reports, according to which the binding of estrogen group compounds to polymers depends on several different types of interactions<sup>42</sup> and might be based on chemisorption.<sup>22</sup> However, of these, the hydrogen bonding plays a key role.

In this work, porous adsorbent filters were fabricated from polymer powders and hybrid materials using selective laser sintering. The polymer powder withstands partial melting without negative effects on the ability of polymers to bind hormones. Furthermore, hormones captured by the filter can be easily removed by simple methanol washing, allowing the reuse of 3D-printed filters. The kinetics studies showed that results obtained were in range with the previous studies<sup>22</sup> and equilibria obtained with pseudo-second order were around 35, 32 and 37  $\mu\text{g g}^{-1}$  for E1, E2 and EE2, respectively.

Although 3D printing provides an excellent tool for modifying the porosity and flow-through properties of the adsorption filter, work is still needed to improve the efficiency and selectivity of filters. In the end, the filter's efficiency depends on the polymeric material. Further improvement of the adsorption capabilities includes modifying functional groups of polymers or adding powerful adsorbent components to the printed filter, as was demonstrated in this work. However, in the latter technique, the adsorbing additive must be selected so that the printed filter can be regenerated and reused.

The amount of different types of plastic residues and plastic waste in our environment is still increasing due to increased global consumption, improper waste handling, and lack of efficient recycling methods. Nevertheless, plastics will continue to play an essential role in our daily lives, and therefore, we need to understand the impacts plastic residues and microplastics can have on our environment. Similarly, we need to find new ways to recycle and reutilize plastic waste to create additional value for already highly processed material.

## Author contributions

Janne Frimodig: conceptualization, methodology, investigations, writing – original draft. Matti Haukka: writing – review & editing, supervision.



## Conflicts of interest

There are no conflicts to declare.

## Acknowledgements

The research was funded by LIFE21-IPE-FI-PlastLIFE/101069513. The PlastLIFE project is co-funded by the European Union. Views and opinions expressed are however those of the authors only and do not necessarily reflect those of the European Union or CINEA. Neither the European Union nor the granting authority can be held responsible for them.

## References

- 1 S. Jobling, M. Nolan, C. R. Tyler, G. Brightly and J. P. Sumpter, *Environ. Sci. Technol.*, 1998, **32**, 2498–2506.
- 2 C. K. Gadupudi, L. Rice, L. Xiao and K. Kantamaneni, *Sci.*, 2019, **1**, 15.
- 3 M. Adeel, X. Song, Y. Wang, D. Francis and Y. Yang, *Environ. Int.*, 2017, **99**, 107–119.
- 4 M. Kostich, R. Flick and J. Martinson, *Environ. Pollut.*, 2013, **178**, 271–277.
- 5 S. Jobling, D. Casey, T. Rodgers-Gray, J. Oehlmann, U. Schulte-Oehlmann, S. Pawlowski, T. Baunbeck, A. P. Turner and C. R. Tyler, *Aquat. Toxicol.*, 2004, **16**.
- 6 Q.-Q. Zhang, C. Xing, Y.-Y. Cai, X.-T. Yan and G.-G. Ying, *Sci. Total Environ.*, 2021, **772**, 145558.
- 7 Q. Zhang, J.-L. Zhao, G.-G. Ying, Y.-S. Liu and C.-G. Pan, *Environ. Sci. Technol.*, 2014, **48**, 7982–7992.
- 8 C. Pironi, M. Ricciardi, A. Proto, P. M. Bianco, L. Montano and O. Motta, *Water*, 2021, **13**, 1347.
- 9 X. Yang, X. He, H. Lin, X. Lin, J. Mo, C. Chen, X. Dai, D. Liao, C. Gao and Y. Li, *Sci. Total Environ.*, 2021, **751**, 141766.
- 10 S. Lavrić, M. Zapater-Pereyra and M. L. Mancini, *Water, Air, Soil Pollut.*, 2017, **228**, 251.
- 11 Y. Wang, X. Wang, M. Li, J. Dong, C. Sun and G. Chen, *Int. J. Environ. Res. Public Health*, 2018, **15**, 269.
- 12 S. Wang, L. Li, S. Yu, B. Dong, N. Gao and X. Wang, *Chem. Eng. J.*, 2021, **406**, 126722.
- 13 A. J. Semião and A. I. Schäfer, *J. Membr. Sci.*, 2013, **431**, 244–256.
- 14 R. Waliullah, A. I. Rehan, M. E. Awual, A. I. Rasee, M. C. Sheikh, M. S. Salman, M. S. Hossain, M. M. Hasan, K. T. Kubra, M. N. Hasan, H. M. Marwani, A. Islam, M. M. Rahman, M. A. Khaleque and M. R. Awual, *J. Mol. Liq.*, 2023, **388**, 122763.
- 15 M. S. Salman, M. N. Hasan, M. M. Hasan, K. T. Kubra, M. C. Sheikh, A. I. Rehan, R. Waliullah, A. I. Rasee, M. E. Awual, M. S. Hossain, A. K. Alsukaibi, H. M. Alshammari and M. R. Awual, *J. Mol. Struct.*, 2023, **1282**, 135259.
- 16 P. Schröder, B. Helmreich, B. Škrbić, M. Carballa, M. Papa, C. Pastore, Z. Emre, A. Oehmen, A. Langenhoff, M. Molinos, J. Dvarioniene, C. Huber, K. P. Tsagarakis, E. Martinez-Lopez, S. M. Pagano, C. Vogelsang and G. Mascolo, *Environ. Sci. Pollut. Res.*, 2016, **23**, 12835–12866.
- 17 A. Tufail, W. E. Price, M. Mohseni, B. K. Pramanik and F. I. Hai, *J. Water Process Eng.*, 2021, **40**, 101778.
- 18 E. C. Smith and A. Turner, *Sci. Total Environ.*, 2020, **733**, 138802.
- 19 G. Liu, J. Wang, M. Wang, R. Ying, X. Li, Z. Hu and Y. Zhang, *Sci. Total Environ.*, 2022, **818**, 151685.
- 20 E. Lahtinen, M. M. Hänninen, K. Kinnunen, H. M. Tuononen, A. Väisänen, K. Rissanen and M. Haukka, *Adv. Sustainable Syst.*, 2018, **2**, 1800048.
- 21 J. Frimodig, A. Autio, E. Lahtinen and M. Haukka, *3D Print. Addit. Manuf.*, 2023, **10**, 1122–1129.
- 22 Y. Leng, W. Wang, H. Cai, F. Chang, W. Xiong and J. Wang, *Sci. Total Environ.*, 2023, **858**, 159803.
- 23 Q. Chen, A. Allgeier, D. Yin and H. Hollert, *Environ. Int.*, 2019, **130**, 104938.
- 24 E. Lahtinen, E. Kukkonen, J. Jokivartio, J. Parkkonen, J. Virkajärvi, L. Kivijärvi, M. Ahlskog and M. Haukka, *ACS Appl. Energy Mater.*, 2019, **2**, 1314–1318.
- 25 S. Yuan, D. Strobbe, J.-P. Kruth, P. Van Puyvelde and B. Van der Bruggen, *J. Membr. Sci.*, 2017, **525**, 157–162.
- 26 T. Koziar, *3D Print. Addit. Manuf.*, 2020, **7**, 126–138.
- 27 G. Flodberg, H. Pettersson and L. Yang, *Addit. Manuf.*, 2018, **24**, 307–315.
- 28 Z. Zhu and C. Majewski, *Mater. Des.*, 2020, **194**, 108937.
- 29 R. Li, S. Yuan, W. Zhang, H. Zheng, W. Zhu, B. Li, M. Zhou, A. Wing-Keung Law and K. Zhou, *ACS Appl. Mater. Interfaces*, 2019, **11**, 40564–40574.
- 30 E. Lahtinen, E. Kukkonen, V. Kinnunen, M. Lahtinen, K. Kinnunen, S. Suvanto, A. Väisänen and M. Haukka, *ACS Omega*, 2019, **4**, 16891–16898.
- 31 C. Tizaoui, S. B. Fredj and L. Monser, *Chem. Eng. J.*, 2017, **328**, 98–105.
- 32 M. S. Moshoeshoe, Nadiye-Tabbiruka and V. Obuseng, *Am. J. Mater. Sci.*, 2017, **7**, 196–221.
- 33 A. I. Schäfer, L. D. Nghiem and T. D. Waite, *Environ. Sci. Technol.*, 2003, **37**, 182–188.
- 34 C. Mejías, J. Martín, J. L. Santos, I. Aparicio and E. Alonso, *Trends Environ. Anal. Chem.*, 2021, **30**, e00125.
- 35 A. I. Schäfer, I. Akanyeti and A. J. Semião, *Adv. Colloid Interface Sci.*, 2011, **164**, 100–117.
- 36 L. Braeken, R. Ramaekers, Y. Zhang, G. Maes, B. V. d. Bruggen and C. Vandecasteele, *J. Membr. Sci.*, 2005, **252**, 195–203.
- 37 L. J. Tan, W. Zhu and K. Zhou, *Adv. Funct. Mater.*, 2020, **30**, 2003062.
- 38 A. Hurwitz and S. Liu, *J. Pharm. Sci.*, 1977, **66**, 624–627.
- 39 P. A. Neale, M. Mastrup, T. Borgmann and A. I. Schäfer, *J. Environ. Monit.*, 2010, **12**, 311–317.
- 40 C. Extrand, *J. Colloid Interface Sci.*, 2002, **248**, 136–142.
- 41 F. Esmaeeli, S. A. Gorbani and N. Moazezi, *Int. J. Environ. Res.*, 2017, **11**, 695–705.
- 42 T. R. Sahoo and B. Prelot, *Nanomaterials for the Detection and Removal of Wastewater Pollutants*, 2020, pp. 161–222.

